

Luminescence Quenching of Ruthenium(II)–Tris(phenanthroline) by Cobalt(III)–Tris(phenanthroline) Bound to the Surface of Starburst Dendrimers

Daniel ben-Avraham and L. S. Schulman

Clarkson Institute of Statistical Physics (CISP) and Department of Physics, Clarkson University, Potsdam, New York 13699-5820

Stefan H. Bossmann*

Lehrstuhl für Umweltmesstechnik am Engler-Bunte-Institut der Universität Karlsruhe, 76128 Karlsruhe, Germany

Claudia Turro

Department of Chemistry, Ohio State University, Columbus, Ohio 43210-1185

Nicholas J. Turro

Department of Chemistry, Columbia University, New York, New York 10027

Received: November 10, 1997; In Final Form: April 16, 1998

We have conducted a statistical analysis of luminescence quenching of the photoexcited sensitizer $[\text{Ru}(\text{phen})_3]^{2+}$ by $[\text{Co}(\text{phen})_3]^{3+}$ on the surface of starburst dendrimer polyanions (SBD generations 3.5–6.5). Our analysis is based on an extension of the random-deposition model, previously developed for the “one-dimensional” case of DNA. Our goal is to deduce the interaction distance (L) characteristic of the photoelectron transfer in the quenching process. The statistical analysis yields the surprising result that the electron donor and acceptor metal complexes do not bind randomly on the SBD’s surfaces but that they tend to be found next to one another. The energy of attraction, $\epsilon \approx 2.9k_{\text{B}}T$, is nearly equal for all four generations of dendrimers tested. We argue that the attraction stems from hydrophobic interactions. The clustering of sensitizers and acceptors results in an increase of luminescence quenching which in the absence of the present analysis (and in particular with a random binding assumption) might erroneously have been attributed to a longer range of electron transfer.

1. Introduction

The study of microheterogeneous and heterogeneous structures through their interaction with metal complexes has been successfully pursued for the past two decades and is today a widely accepted and highly developed method.¹ The technique relies on the dependence of luminescence lifetimes and intensities in the ³MLCT (metal to ligand charge transfer) excited states of ruthenium(II)–polypyridyl complexes upon their local microenvironment and on the effect of quenchers such as cobalt(III)–polypyridyl complexes.² Examples of (micro)heterogeneous structures thus studied include DNA,³ proteins,⁴ starburst dendrimers,⁵ heterogeneous photocatalysts for water⁶ and CO₂ reduction,⁷ and humic substances.⁸ Photophysical experiments yield valuable information about the binding constants of the metal complexes to (micro)heterogeneous surfaces, intercalation into these hosts (when present), the structure and extension of the double layer around the polyelectrolytes surfaces, and the electron transfer rate constants.⁹

The body of work just alluded to represents the triumph of a major paradigm¹⁰ in the field of photophysics and photochemistry.¹¹ However, scientific conclusions depend on the underlying mechanical model. Misinterpretations may arise when experimental data are analyzed within an overly simplified or incorrect mechanistic scheme.⁸ Therefore, it is imperative to

choose the underlying models carefully. This is best achieved by analyzing the same set of experimental data according to different paradigms and then comparing their conclusions, and by selecting models which contain as few assumptions as possible.

Recently, we have developed a statistical method for the analysis of photoelectron transfer quenching in metal complexes of sensitizers and acceptors bound to DNA.¹² The analysis is based only on the assumption that the binding of metal complexes to DNA may be modeled by the random deposition of segments (the complexes) on a one-dimensional lattice (DNA). The electron-transfer range, *i.e.*, the typical distance within which quenching may take place, plays a central role in this statistical analysis. Thus, the influence of the DNA medium on the electron transfer could be deduced.¹² Indeed, our analysis afforded us new insights which in the meantime have been corroborated by others:¹³ (1) The computed density of the adsorbed metal complexes, $0.8834 < \rho < 1.3396$, was significantly larger than the maximum density of “jamming” with random deposition, $\rho_{\text{jamming}} = 0.8083$. This indicates clustering of the metal complexes. (2) The electron-transfer range exceeds the combined radii of the metal complexes by only 10–15%.

Starburst dendrimers (SBDs) provide an ideal system for the development of statistical analyses of luminescence quenching

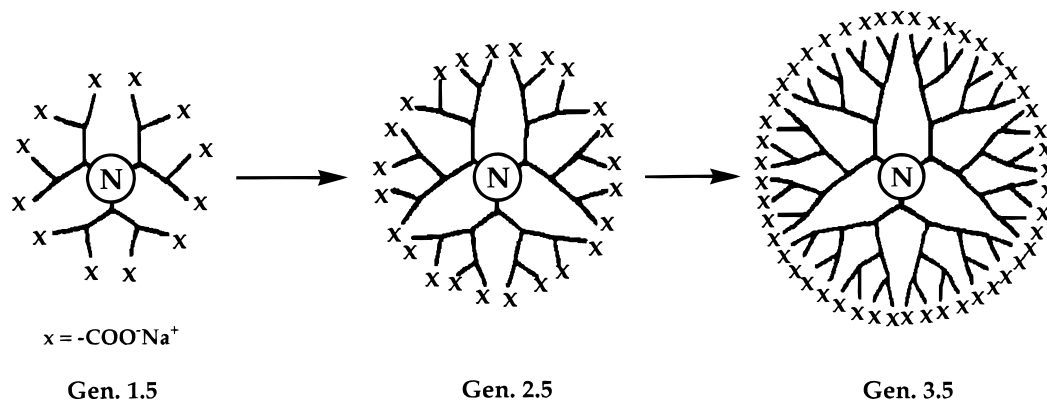


Figure 1. Schematic representation of the starburst dendrimer.

TABLE 1: SBD Parameters: Generation (G), Molecular Weight (MW), Diameter (d), Number of Carboxylate Functions (n), Average Separation, and Surface Area

G	MW	d ($\times 10^9$ m)	n -COOH	separation ($\times 10^9$ m)	surface area ($4\pi r^2 \times 10^{16}$ m 2)
0.5	924	2.79	6	1.24	0.245
1.5	2173	3.62	12	1.28	0.412
2.5	4671	4.83	24	1.27	0.733
3.5	9668	6.61	48	1.26	1.367
4.5	19661	8.79	96	1.15	2.433
5.5	39648	10.39	192	1.03	3.941
6.5	79621	12.68	384	0.98	4.987

in two dimensions. SBDs are a class of macromolecules of known molecular composition and of well-defined size.¹⁴ The SBDs that we employed in our experiments are PAMAMs [poly(amidoamine)] consisting of a nitrogen core atom with three radiating branches of $\text{CH}_2\text{CH}_2\text{CONHCH}_2\text{CH}_2\text{N}$. In subsequent generations each of these branches is attached to two similar branches. The branches at the external surface of the SBD macromolecules may be terminated at a carboxylic–methyl ester stage. When hydrolysis of these esters is performed one obtains the so-called “half generations,” $n.5$. As a consequence, the $n.5$ generations feature a well-defined number of sodium–carboxylate functions ($-\text{COO}^-\text{Na}^+$). In Table 1, we summarize the molecular weights, diameters, number of carboxylate functions, and surface areas of different SBD generations (see also Figure 1).

SBDs have been studied extensively by photophysical methods and classic parameters such as binding and quenching constants at the SBD’s surfaces have been obtained.⁵ Our luminescence experiments involve the well-known sensitizer ruthenium(II)–tris(phenanthroline) $[\text{Ru}(\text{phen})_3]^{2+}$ and the electron acceptor $[\text{Co}(\text{phen})_3]^{3+}$ (Figure 2). Both metal complexes are nearly equal in size: their diameters are^{2a} 12.2 Å.

The development of a two-dimensional random deposition model should yield a quantitative description of luminescence quenching. In that respect, the electron-transfer range between photoexcited sensitizers $[\text{Ru}(\text{phen})_3]^{2+}$ and electron acceptors $[\text{Co}(\text{phen})_3]^{3+}$ are of special interest. Another important question is whether the binding of the metal complexes to the SBDs takes place in a purely random fashion, or if there is preferential binding of some species, or correlated binding of donor–acceptor pairs, or clustering of three or more complexes, etc.

In our statistical analysis of the binding of ruthenium(II)– and cobalt(III)–polypyridyl complexes on DNA and in the corresponding analysis of the binding on SBDs, one must keep in mind that the actual binding mechanisms involved are quite different. Whereas in the interaction of metal–polypyridyl complexes and DNA both intercalation and surface binding are

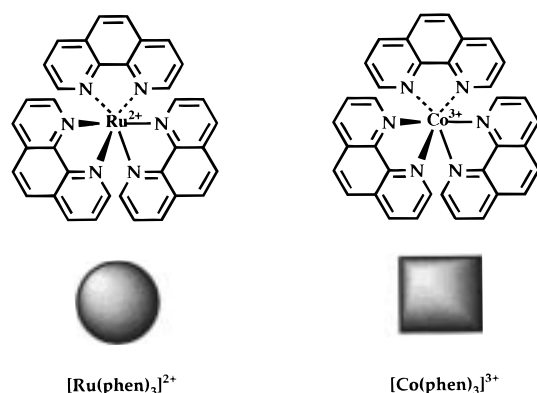


Figure 2. Chemical structure of $[\text{Ru}(\text{phen})_3]^{2+}$ and $[\text{Co}(\text{phen})_3]^{3+}$.

observed,³ the rigid structure of the SBD macromolecules permits only surface binding of the relatively big metal–polypyridyl complexes.^{1a} Therefore, different electron transfer ranges (L) may be observed in these two systems. However, this does not affect the validity of the statistical tools we use, and indeed the absence of dependence on mechanistic detail may be considered a virtue of this statistical method.

2. Description of the Experiment

2.1. Materials. $[\text{Ru}(\text{phen})_3]^{2+}$ and 1,10-phenanthroline, Sephadex G 50, EtOH, and DMF (solvents, ACS grade) as well as PAMAM 3.5–4.5 SBDs were purchased from Aldrich (dissolved in MeOH). Additional starburst dendrimers were a gift from the Michigan Molecular Institute for which we are indebted to Prof. D. Tomalia. The chemicals were used as received, with the exception of SBD solutions in MeOH, which were dried in high vacuum prior to use. Deionized water (Millipore and UHQ II) was used in all quenching experiments.

2.2. Methods. The photophysical experiments were performed in air-equilibrated deionized water solutions. The pH of the bulk solution was 8.4 ± 0.1 , and the temperature was held at 298 ± 1 K. The concentrations of the SBDs, $[\text{Ru}(\text{phen})_3]^{2+}$, and $[\text{Co}(\text{phen})_3]^{3+}$ were optimized¹⁶ in order to ensure that all metal complexes were bound to the SBD–polyelectrolyte particles. Indeed, photoelectron transfer rates in our experiments were of the order of $k_q \approx 10^7$ – 10^6 s $^{-1}$. These unimolecular rate constants are in contrast with bimolecular rates of the order of $k_q \approx 5 \times 10^8$ mol $^{-1}$ L s $^{-1}$ which are typical when a fraction of sensitizers and quenchers remains in solution. The concentrations used and the experimental data are given in the Appendix.

2.3. Instrumentation. The single-photon-counting setup employed in the experiment has been described elsewhere.¹⁷

The decay traces were analyzed by use of a computer program generously provided by Prof. F. C. De Schryver of the University of Leuven, Belgium. Steady-state emission spectra were recorded on a Perkin-Elmer (LS-5) instrument. Additional stationary and time-resolved single-photon-counting experiments were performed using an FL900CDT and FS900CDT SPC spectrometer from Edinburgh Analytical Instruments. We thank Prof. A. M. Braun for the use of his facilities at the University of Karlsruhe.

2.4. Data Collection. Not only does our statistical analysis rely on the precision of the data collected, but the selection of the “time window” of the experiments has significant bearing on what sort of conclusions can be drawn. In general, when the metal complexes are close enough to each other for a reaction to occur, electron-transfer processes proceed in a characteristic time much shorter than a nanosecond.² On the surface of a polyelectrolyte, diffusion processes are responsible for the reaction kinetics. In a purely diffusion-controlled photoreaction system, the luminescence decrease of a sensitizer under continuous irradiation due to the effect of electron transfer quenching is expressed by the classic Stern–Volmer equation:¹⁸

$$I_0/I = 1 + k_q\tau_0[Q] \quad (1a)$$

where I_0 is the luminescence intensity without addition of the quencher, I luminescence intensity as a function of quencher concentration, τ_0 luminescence lifetime without addition of the quencher, $[Q]$ concentration of the quencher (mol L^{-1}), and k_q bimolecular quenching constant ($\text{mol}^{-1} \text{L s}^{-1}$).

In analogy to eq 1a, the time-resolved luminescence quenching, and thus the contribution of diffusion-controlled quenching processes to the total quenching, can be calculated using:¹⁷

$$\tau_0/\tau = 1 + k_q\tau_0[Q] \quad (1b)$$

where τ is the luminescence lifetime as a function of quencher concentration.

The luminescence lifetimes of $[\text{Ru}(\text{phen})_3]^{2+*}$ bound to the surfaces of generation- $n.5$ SBDs is of the order of 400–700 ns, and in the absence of $[\text{Co}(\text{phen})_3]^{3+}$ the luminescence decay is monoexponential. Furthermore, no experimental evidence has been found for the binding of two $[\text{Ru}(\text{phen})_3]^{2+}$ metal complexes next to each other at the SBD $n.5$ surfaces. It is well-known that such a clustering of sensitizers would cause a significant splitting or shift of their $\pi-\pi^*$ transitions.⁷

During the relatively long lifetime of $[\text{Ru}(\text{phen})_3]^{2+*}$ the distribution of the metal complexes on the SBD surface changes, due to diffusion. Therefore, the picture from the quenching experiment is somewhat blurry if one uses data from intensity quenching only. This effect is essentially the same as when the aperture of a camera is left open for too long. However, contributions of the diffusion process to quenching can be accounted for by measuring (τ_0/τ) and subtracting it from the intensity quenching (I_0/I) . The result is the $(I_0/I)_{\text{snapshot}}$ data, which can be used as reliable input data for the development of two-dimensional random deposition methods:

$$\left(\frac{I_0}{I}\right)_{\text{snapshot}} = \frac{I_0}{I} - \frac{\tau_0}{\tau} + 1 \quad (2)$$

Depending on the response time of the single-photon counter used in our time-resolved experiments, all diffusion-controlled processes, which occur at times longer than 1 ns, can be subtracted.

Note that the concentrations of quenchers and sensitizers at the surfaces of the SBDs are different from the concentrations calculated for purely homogeneous systems. Therefore, bimolecular quenching constants in microheterogeneous and heterogeneous systems, which are calculated by assuming a random distribution of sensitizers and quenchers, differ from their “true” values by several orders of magnitude.

Another interesting issue is concerned with possible deviations of starburst dendrimer macromolecules from ideal shapes. Any deviation of the SBDs from spherical could result in different quenching behavior. The earlier generations of the PAMAM dendrimers (1.5–3.5) possess in general a disklike shape, whereas the later generations (4.5–9.5) have a more or less globelike shape. The result of our molecular modeling simulations using the commercially available program Chemdraw 3D is shown in Figure 3. The SBDs become more globelike with increasing generation number. Given the size of the molecular probes employed in our experiments, we may consider generations 4.5 and larger as spherical. The driving force for the photoelectron transfer between $[\text{Ru}(\text{phen})_3]^{2+*}$ and $[\text{Co}(\text{phen})_3]^{3+}$ is 1.20 V.¹⁹

3. Theory and Results

3.1. The Random-Deposition Approach. In the following, we use the same terminology as in our work with DNA.¹² Accordingly, we term the sensitizers ($[\text{Ru}(\text{phen})_3]^{2+}$) and the quenchers ($[\text{Co}(\text{phen})_3]^{3+}$) “circles” and “squares”, respectively.

The variables used here are defined as follows: ν_c , average number of circles on each SBD molecule; ν_s , average number of squares on each SBD molecule; ρ_c , concentration of circles in solution; ρ_s , concentration of squares in solution; ρ_{SBD} , concentration of SBDs in solution; L , photoelectron transfer interaction range; and I , luminescence intensity.

From the rate constants and the concentrations involved, as well as experimental evidence,²⁰ it can be assumed that all complexes are bound to the SBD surface. Thus, the average number of squares, ν_s , and circles, ν_c , adsorbed on the surface of each SBD particle is

$$\nu_{s,c} = \rho_{s,c}/\rho_{\text{SBD}} \quad (3)$$

The intensity quenching $(I_0/I)_{\text{snapshot}}$ may be computed given the following assumptions:

1. The effect of a single square at distance r from a circle is to reduce the intensity by $(1 - e^{-r/L})$. This is the same assumption as for DNA.¹² It is not essential and may be relaxed without affecting our conclusions.

2. The action of a square is not limited to the nearest circle. It can act on all circles (on the same SBD), without interference. Also, squares do not interfere with each other. This simplifies the model considerably and is an even safer assumption for SBDs than it is for DNA, since in the two-dimensional geometry the electrons can find alternate routes past intervening objects.

3. The distribution of circles and squares on the SBD surface is random; *i.e.*, there are no attractive or repulsive interactions. This is the weakest assumption, and our most important qualitative conclusion is that it turns out to be wrong!

In the experiments under consideration, ν_s and ν_c are relatively small, so we may use Poisson statistics. With the assumption of no interactions, the probability of having n_s squares and n_c circles on the surface of a single SBD is

$$p(n_s, n_c) = \left(\frac{\nu_s^{n_s}}{n_s!} e^{-\nu_s}\right) \left(\frac{\nu_c^{n_c}}{n_c!} e^{-\nu_c}\right) \quad (4)$$

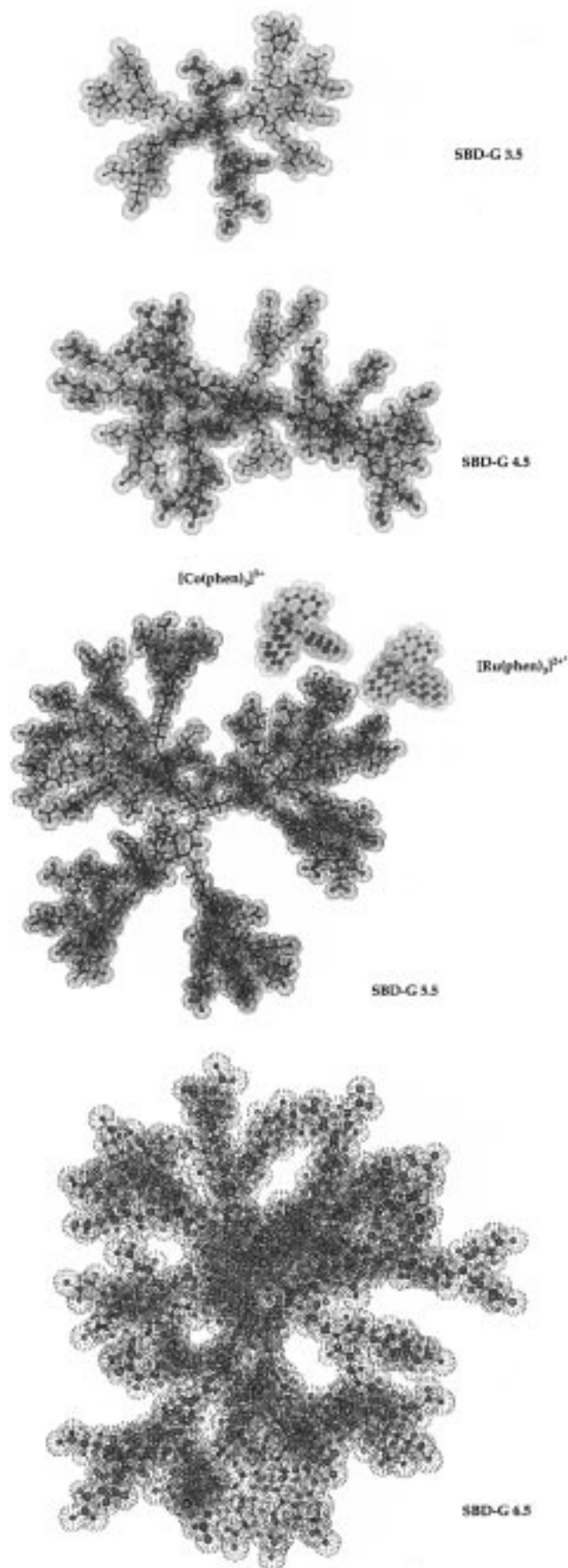


Figure 3. Computer simulations of SBDs configurations.

Let the average intensity emitted by a SBD carrying n_s squares and n_c circles be I_{n_s, n_c} . The effect of a square on a single circle

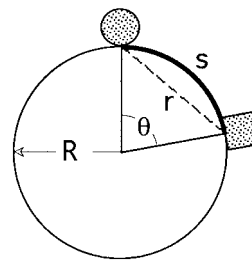


Figure 4. Diagram used for the computation of the attenuation factor, eq 8. The electron-transfer distance s between circles and squares is measured on the surface of the SBD (heavy line). A different computation may be based on the shortest distance r (broken line), but it does not change the conclusions.

is to reduce the intensity by a factor $\alpha < 1$; $I_{1,1} = \alpha I_{0,1}$. Since the effect of several squares is to quench emission independently, $I_{n_s,1} = \alpha^{n_s} I_{0,1}$; if more than one circle is on the SBD the intensity becomes

$$I_{n_s, n_c} = n_c \alpha^{n_s} I_{0,1} \quad (5)$$

Given N SBDs in solution the total intensity is

$$I = N \sum_{n_s=0}^{\infty} \sum_{n_c=0}^{\infty} p(n_s, n_c) I_{n_s, n_c} = N \nu_c J_{0,1} e^{\nu_s (\alpha - 1)} \quad (6)$$

I_0 is obtained by substituting $\nu_s = 0$, so

$$(I_0/I)_{\text{snapshot}} = e^{(1-\alpha)\nu_s} \quad (7)$$

The attenuating factor α depends on the geometry of the problem, as well as on our assumption for the quenching effect of a single square. α represents the quenching of a single square, averaged over all its possible locations. For example, consider a circle and a square on a SBD of radius R . Assume that the quenching factor depends on the distance s measured along the surface of the SBD (Figure 4); it is therefore $(1 - e^{-s/L})$. Averaging over all possible locations of the square we get

$$\alpha = \frac{\int_0^{\pi R} (1 - e^{-s/L}) 2\pi R \sin(s/R) ds}{\int_0^{\pi R} 2\pi R \sin(s/R) ds} = 1 - \frac{1 + e^{-\pi R/L}}{2[1 + (R/L)^2]} \quad (8)$$

From eq 7 we see that

$$\ln[(I_0/I)_{\text{snapshot}}] = (1 - \alpha)\nu_s \quad (9)$$

and the data indeed show this linear dependence of the logarithm of the intensity upon ν_s for SBDs of all the generations tested (Figure 5).

The radius R of n_s SBDs is known from size-exclusion chromatography experiments (see Table 1). These measured radii are in good agreement with the ones obtained from molecular modeling. Having determined α , we are then able to compute the electron transfer range, L , from eq 8. This analysis yields $L = 65, 100,$ and 300 \AA , for generations 6.5, 5.5, and 4.5, respectively (Table 2). The variation of L with SBD size indicates a flaw in this model. One could argue that other assumptions about the quenching capacity of a square would yield a more constant L . We have also tried a model where the quenching length r is the shortest distance between circle and square, cutting through the SBD's bulk (Figure 4). This gave essentially no improvement. Moreover, for generation

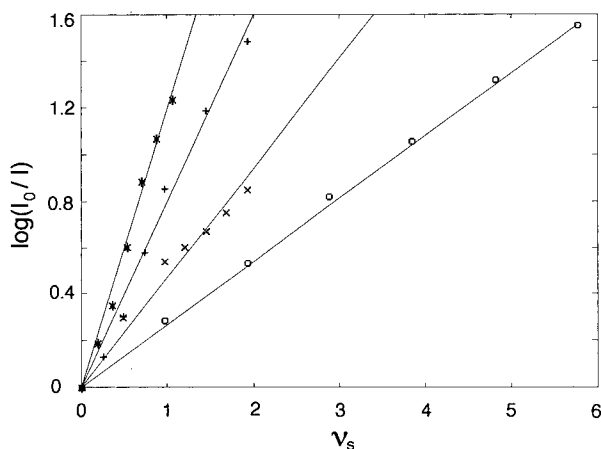


Figure 5. Experimental data for $\ln(I/I_0)$ vs ν_s , for SBD generations 3.5 (*), 4.5 (+), 5.5 (\times), and 6.5 (O). The solid lines represent the best linear fit. The slopes are summarized in Table 2.

TABLE 2: Summary of Theoretical Analysis of the Data^a

SBD generation	slope	L (Å)	ϵ ($k_B T$)
3.5	1.20	undefined	2.8
4.5	0.80	300	2.9
5.5	0.47	100	2.9
6.5	0.27	65	3.0

^a The slope in column 2 is the best fit to the experimental data of Figure 5. It may be interpreted either as $1 - \alpha$ (eq 9) or as $\ln[(M - m - 1) + m\omega]/[M - m - 1]$ (eq 10). Column 3 represents the electron-transfer range computed from α with the first interpretation, while column 4 lists the energetic advantage for circles and squares to land next to each other as computed from ω in the latter interpretation.

3.5 we find that the slope $(1 - \alpha)$ in eq 9 turns out to be about 1.2, significantly larger than (the maximum physical value) one! That is, there is more quenching than our model can accommodate; it cannot be explained with *any* theory of α , nor with alternative forms of the quenching factor $(1 - e^{-r/L})$. Our conclusion is that the least supportable assumption, that of no interaction between squares and circles in the adsorption process, is wrong. The extra quenching comes from the propensity of squares to land next to circles.

We know from numerous experiments on the surfaces of micelles and starburst dendrimers that the excited state redox potential of $[\text{Ru}(\text{phen})_3]^{2+*}$ as well as the redox potential of $[\text{Co}(\text{phen})_3]^{3+}$ is almost not affected by a change of the interacting polyanionic structure. Therefore, we are justified in assuming that the potential difference between the metal complexes would not vary from one SBD generation to the next and that the electron transfer range L is indeed constant. Although we have considered that possibility, experiments also show that *n*.5-PAMAM SBDs do not support electron transfer through their interior structures.

3.2. Interactions between the Adsorbed Metal Complexes. Having shown that a random-deposition model for the interaction of sensitizers and quenchers does not yield logical results, let us see how interactions in the adsorption process can explain the data. Here is a simple model that works. Assume the following:

1. There is an energetic advantage of magnitude ϵ for squares to adsorb right next to a circle (as opposed to further away), represented by the Boltzmann factor $\omega = e^{\epsilon/k_B T}$.

2. If a square adsorbs right next to a circle it quenches luminescence completely, but if it lands some distance away it has no effect.

Given the size of circles and squares and the size of surface groups on the SBD (Table 1), it is reasonable to assume that

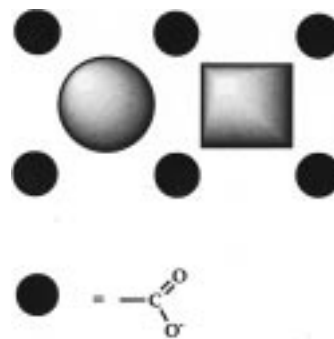


Figure 6. Binding of $[\text{Ru}(\text{phen})_3]^{2+}$ and $[\text{Co}(\text{phen})_3]^{3+}$ on the SBD surface.

only one circle or square may adsorb on each surface group or in the junction between adjacent groups. Since the circles and squares possess +2 and +3 charges, respectively, the best charge compensation by the negative SBD headgroups ($-\text{COO}^-$) would be achieved when a circle and a square are bound next to each other as shown in Figure 6. In this way, the overall +5 charge from the adjacent metal complexes is compensated by the six surrounding anionic carboxylate groups.

Let the number of surface groups be M , and let the number of nearest groups to an adsorbed circle be m . Since a square is ω times more likely to adsorb to one of the m nearest sites, rather than to one of the remaining $M - m - 1$ sites, the probability that it does not adsorb to any of the m nearest sites is $p = (M - m - 1)/[m\omega + (M - m - 1)]$. A circle will fluoresce only in the event that there are no squares in any of its nearest sites. Thus, if ν_s squares are adsorbed, the probability of fluorescence drops to p^{ν_s} , and $(I_0/I)_{\text{snapshot}} = p^{-\nu_s}$, or

$$\ln(I_0/I)_{\text{snapshot}} = \nu_s \ln \frac{(M - m - 1) + m\omega}{M - m - 1} \quad (10)$$

This is again a linear expression in ν_s , except that here the coefficient may become as large as necessary, simply by adjusting the attractive potential, ϵ . With this model we can explain the data consistently. Using the number of surface groups in Table 1, and assuming $m = 6$, we get $\epsilon \approx 2.9k_B T$ (at 298 K) for all generations tested (Table 2). The magnitude of the attractive potential is typical of hydrophobic interactions ($1 - 10k_B T$). We suspect that hydrophobic interactions are indeed responsible for the clustering effect. In particular, it seems likely that the carboxylate groups of the dendrimer's structure serve as gegenions²¹ and therefore the positive charges of both ruthenium(II) and cobalt(III) complexes are neutralized so that the hydrophobic effect can take place.

4. Conclusions

Aiming at a quantitative analysis of the photoelectron transfer between the excited sensitizer $[\text{Ru}(\text{phen})_3]^{2+*}$ and the electron acceptor quencher $[\text{Co}(\text{phen})_3]^{3+}$, adsorbed at the surfaces of *n*.5 SBD generations (3.5–6.5), we have developed a random-deposition model for sensitizer/quencher interactions on a two-dimensional surface. This approach is based on the assumption of random distributions of both types of metal complexes on the SBDs surfaces. However, this led to a contradiction regarding the electron-transfer range L : the analysis yielded different ranges for generations 4.5, 5.5, and 6.5 and was unable to account for the data from generation 3.5.

We were thus compelled to consider a model of mutual attraction between the metal complexes. In this second analysis we have omitted the parameter L , replacing it by short-range

TABLE 3

	mol L ⁻¹	I ₀ /I	τ ₀ /τ	I ₀ /I - τ ₀ /τ + 1
SBD G 3.5	4.29 × 10 ⁻⁴			
[Ru(phen) ₃] ²⁺	3.30 × 10 ⁻⁴			
[Co(phen) ₃] ³⁺	0	1	1	1
	0.75 × 10 ⁻⁴	1.323	1.116	1.207
	1.50 × 10 ⁻⁴	1.58	1.157	1.423
	2.25 × 10 ⁻⁴	2.124	1.294	1.830
	3.00 × 10 ⁻⁴	2.83	1.413	2.417
	3.75 × 10 ⁻⁴	3.388	1.472	2.916
	4.50 × 10 ⁻⁴	4.06	1.624	3.436
SBD G 4.5	1.04 × 10 ⁻⁴			
[Ru(phen) ₃] ²⁺	1.00 × 10 ⁻⁵			
[Co(phen) ₃] ³⁺	0	1	1	1
	2.50 × 10 ⁻⁵	1.218	1.075	1.143
	5.00 × 10 ⁻⁵	1.457	1.102	1.355
	7.50 × 10 ⁻⁵	1.971	1.188	1.783
	1.00 × 10 ⁻⁴	2.521	1.168	2.352
	1.50 × 10 ⁻⁴	3.456	1.182	3.274
	2.00 × 10 ⁻⁴	4.590	1.178	4.412
SBD G 5.5	5.20 × 10 ⁻⁵			
[Ru(phen) ₃] ²⁺	1.00 × 10 ⁻⁵			
[Co(phen) ₃] ³⁺	0	1	1	1
	2.50 × 10 ⁻⁵	1.445	1.098	1.347
	5.00 × 10 ⁻⁵	1.80	1.084	1.716
	6.25 × 10 ⁻⁵	1.90	1.075	1.825
	7.50 × 10 ⁻⁵	2.01	1.048	1.962
	8.75 × 10 ⁻⁵	2.182	1.055	2.127
	1.00 × 10 ⁻⁴	2.41	1.066	2.344
SBD G 6.5	1.30 × 10 ⁻⁵			
[Ru(phen) ₃] ²⁺	1.00 × 10 ⁻⁵			
[Co(phen) ₃] ³⁺	0	1	1	1
	1.25 × 10 ⁻⁵	1.59	1.255	1.335
	2.50 × 10 ⁻⁵	1.92	1.215	1.705
	3.75 × 10 ⁻⁵	2.48	1.207	2.273
	5.00 × 10 ⁻⁵	3.06	1.191	2.869
	6.25 × 10 ⁻⁵	3.897	1.152	3.745
	7.50 × 10 ⁻⁵	4.86	1.120	4.740

quenching. We have done this so that there would be only one fitting parameter, the energetic attraction potential ϵ , rather than L , in order to sharpen our conclusions. The attractive potential of $2.9k_B T$ that we have found for all four $n.5$ generations of SBDs studied is consistent with a hydrophobic interaction. We clearly see here the importance of a statistical mechanical analysis of the experimental data. Without this analysis, the clustering of quenchers and sensitizers (and the consequent increase in the observed luminescence quenching) might easily have been misinterpreted as long-range photoelectron transfer. Clustering in photoluminescence experiments in organic ligands employing metal complexes is not unusual.

Acknowledgment. Financial support from the German Chemical Industry Foundation (VCI), the Deutsche Forschungsgemeinschaft (DFG), the United States National Science Foundation, and NATO is gratefully acknowledged.

References and Notes

(1) (a) Turro, N. J.; Barton, J. K.; Tomalia, D. A. *Acc. Chem. Res.* **1991**, *24*, 332–340. (b) Gehlen, M. H.; De Schryver, F. C. *Chem. Rev.* **1993**, *93*, 199. (c) Kalyanasundaram, K. *Photochemistry in Microheterogeneous Systems*; Academic Press: New York, 1987, and references therein. (d) *Photoinduced Electron Transfer*, Mattay, J., Ed.; Topic in Current Chemistry Series; Springer-Verlag: New York, 1991. (e) Colaneri, M. J.;

Kevan, L.; Schmehl, R. *J. Phys. Chem.* **1989**, *93*, 397. (f) Schmehl, R. H.; Whitten, D. G. *J. Phys. Chem.* **1981**, *85*, 3473.

(2) (a) Juris, A.; Barigelli, F.; Campagna, S.; Balzani, V.; Belser, P.; Zelewsky, A. v. *Coord. Chem. Rev.* **1988**, *84*, 85; (b) Kalyanasundaram, K. *Coord. Chem. Rev.* **1982**, *46*, 159. (c) Kalyanasundaram, K. *Photochemistry of Polypyridine and Porphyrin Complexes*; Academic Press: London, San Diego, New York, 1992.

(3) (a) Purugganan, M. D.; Kumar, C. V.; Turro, N. J.; Barton, J. K. *Science* **1988**, *241*, 1645. (b) Ottaviani, M. F.; Ghatlia, N. D.; Bossmann, S. H.; Turro, N. J.; Barton, J. K.; Dürr, H. *J. Am. Chem. Soc.* **1992**, *114*, 8946–52. (c) Turro, C.; Bossmann, S. H.; Niu, S.; Barton, J. K.; Turro, N. J. *Inorg. Chim. Acta* **1996**, *252*, 333–310. (d) Arkin, M. R.; Stemp, E. D. A.; Turro, C.; Turro, N. J.; Barton, J. K. *J. Am. Chem. Soc.* **1996**, *118*, 2267–2274. (e) Hall, D. B.; Barton, J. K. *J. Am. Chem. Soc.* **1997**, *119*, 5045–5046.

(4) (a) Turro, C.; Zaleski, J. M.; Karabatsos, Y. M.; Nocera, D. G. *J. Am. Chem. Soc.* **1996**, *118*, 6060–6067. (b) Lincoln, P.; Tuite, E.; Norden, B. *J. Am. Chem. Soc.* **1997**, *119*, 1454.

(5) (a) Dvornic, P. R.; Tomalia, D. A. *Macromol. Symp.* **1994**, *1994*, 123–148. (b) Jockusch, S.; Turro, N. J.; Tomalia, D. A. *J. Inf. Rec. Mater.* **1996**, *5*–6. (c) Ottaviani, M. F.; Cossu, E.; Turro, N. J.; Tomalia, D. A. *J. Am. Chem. Soc.* **1995**, *117*, 4387–4398. (d) Ottaviani, M. F.; Turro, N. J.; Jockusch, S.; Tomalia, D. A. *J. Phys. Chem.* **1996**, *100*, 13675–13686. (e) Ottaviani, M. F.; Montalti, F.; Romanelli, M.; Turro, N. J.; Donald A. Tomalia, D. A. *J. Phys. Chem.* **1996**, *100*, 11033–11042. (f) Ottaviani, M. F.; Montalti, F.; Turro, N. J.; Tomalia, D. A. *J. Phys. Chem. B* **1997**, *101*, 158–166. (g) Schwartz, B. L.; Rockwood, A. L.; Smith, R. D.; Tomalia, D. A.; Spindler, R. *Rapid Commun. Mass Spectrom.* **1995**, *9*, 1552–1555. (h) Tomalia, D. A. *Adv. Mater.* **1994**, *6*, 529–539. (i) Tomalia, D. A. *NATO ASI Ser. C Math. Phys. Sci.—Adv. Study Inst.* **1995**, *473*, 21–26.

(6) (a) Bossmann, S. H.; Dürr, H.; Mayer, E. Z. *Naturforsch.* **1993**, *48b*, 369–386. (b) Dürr, H.; Bossmann, S. H.; Beuerlein, A. *J. Photochem. Photobiol. A: Chem.* **1993**, *73*, 233–245.

(7) (a) Schwarz, P.; Bossmann, S. H.; Guldner, A.; Dürr, H. *Langmuir* **1994**, *10*, 4483–4497. (b) Kumar, C. V.; Williams, Z. J. *J. Phys. Chem.* **1995**, *99*, 17632–17639.

(8) Bossmann, S. H. *Kombinierte photophysikalische, Elektronenspinresonanz und analytische Untersuchungen in mikroheterogenen und heterogenen Systemen als Grundlage der Entwicklung phänomenologischer und topologischer Modelle*; Universität Karlsruhe: Karlsruhe, Germany, 1997.

(9) -[9] (a) Murphy, C. J.; Arkin, M. R.; Ghatlia, N. D.; Bossmann, S. H.; Turro, N. J.; Barton, J. K. *Proc. Natl. Acad. Sci. U.S.A.* **1994**, *91*, 5315–5319. (b) Arkin, M. R.; Stemp, E. D. A.; Holmlin, R. E.; Barton, J. K.; Hörmann, A.; Olson, E. J. C.; Barbara, P. F. *Science* **1996**, *273*, 475–479. (c) Arkin, M. R.; Jenkins, Y.; Murphy, C. J.; Turro, N. J.; Barton, J. K. *Adv. Chem. Ser.* **1995**, *246*, 449–470.

(10) Kuhn, T. S. *The Structure of Scientific Revolutions*; University of Chicago Press: Chicago, IL, 1973.

(11) (a) Turro, N. J. *Angew. Chem., Int. Ed. Engl.* **1986**, *25*, 882–901. (b) Turro, N. J. *J. Photochem. Photobiol.—A: Chem.* **1996**, *100*, 53–56. (c) Turro, N. J. *NATO ASI Ser. C Math. Phys. Sci.—Adv. Study Inst.* **1996**, *480*, 429–450.

(12) (a) Schulman, L. S.; Bossmann, S. H.; Turro, N. J. *J. Phys. Chem.* **1995**, *99*, 9283–9292. (b) Bossmann, S. H.; Schulman, L. S. In *Nonequilibrium Statistical Mechanics in One Dimension*; Privman, V., Ed.; Cambridge University Press, Cambridge, UK, 1997; pp 443–460.

(13) Olson, E. J. C.; Hu, D.; Hörmann, A.; Barbara, P. F. *J. Phys. Chem. B* **1997**, *101*, 299–303.

(14) Tomalia, D. A.; Naylor, A. M.; Goddard, W. A. *Angew. Chem., Int. Ed. Engl.* **1990**, *29*, 138–156 and references therein.

(15) (a) Dollimore, L. S.; Gillard, R. D. *J. Chem. Soc., Dalton Trans.* **1973**, 933. (b) Baker, B. R.; Metha, B. D. *Inorg. Chem.* **1965**, *4*, 848. (c) Ohno, T.; Kato, S. *Bull. Chem. Soc. Jpn.* **1971**, *44*, 1527.

(16) Niu, S. Ph.D. Thesis, Columbia University, New York, 1993.

(17) Gopidas, K. R.; Leheny, A. R.; Caminati, G.; Turro, N. J.; Tomalia, D. A. *J. Am. Chem. Soc.* **1991**, *119*, 7335.

(18) Turro, N. J. *Modern Molecular Photochemistry*; University Science Books: Mill Valley, 1991.

(19) $E_{1/2}([\text{Ru}(\text{phen})_3]^{2+/*3+}) = -0.87\text{V}$ (vs NHE); $E_{1/2}([\text{Co}(\text{phen})_3]^{3+}) = +0.33\text{V}$ (vs NHE); see: Turro, C.; Bossmann, S. H.; Niu, S.; Barton, J. K.; Turro, N. J. *Inorg. Chim. Acta* **1996**, *252*, 333–310.

(20) Claudia Turro, Shufang Niu, Stefan H. Bossmann, Donald A. Tomalia and Nicholas J. Turro, *J. Phys. Chem.* **1995**, *99*, 5512–5517.

(21) Turro, N. J.; Khudyakov, I. V. *J. Phys. Chem.* **1995**, *99*, 7654.